

Exciton Regeneration at Polymeric Semiconductor Heterojunctions

Ame C. Morteani, Paiboon Sreearunothai, Laura
M. Herz, Richard H. Friend, and Carlos Silva^y
Cavendish Laboratory, University of Cambridge,
Madingley Road, Cambridge CB3 0HE, United Kingdom

(Dated: 22nd March 2004)

Abstract

Control of the band-edge offsets at heterojunctions between organic semiconductors allows efficient operation of either photovoltaic or light-emitting diodes. We investigate systems where the exciton is marginally stable against charge separation, and show via E-field-dependent time-resolved photoluminescence spectroscopy that excitons that have undergone charge separation at a heterojunction can be efficiently regenerated. This is because the charge transfer produces a geminate electron-hole pair (separation 2.2 ± 3.1 nm) which may collapse into an exciplex and then endothermically ($E_A = 100 \pm 200$ meV) back-transfer towards the exciton.

PACS numbers: 73.20.-r, 73.50.Pz, 78.55.Kz, 78.66.Qn

Efficient optoelectronic devices fabricated with semiconductor polymers often employ heterojunctions between two components in which both the electron affinity and ionization potential are higher in one material than in the other (type II' heterojunctions, see inset of Fig. 1). This configuration is commonly used in photovoltaic diodes to achieve charge generation at the hetero-interface [1, 2, 3]. Typical devices involve a thin film of a blend of hole-accepting and electron-accepting polymers sandwiched between two electrodes. However, some type II polymer blends show low photocurrents and high luminescence quantum yields, leading to very efficient light-emitting diodes [4, 5, 6, 7].

The high luminescence quantum yield is commonly rationalized by the proposition that excitons can be stable at the heterojunction if their Coulombic binding energy is higher than the band edge offsets [4]. In this case, the only process that might occur when an exciton encounters the heterojunction is energy transfer from the material with the larger band gap to the other component. This picture classifies type II heterojunctions into those above and those below a charge-separation threshold, producing high photocurrents or luminescence quantum yields, respectively. This simple classification is incomplete because even systems that show high luminescence efficiencies often also show significant charge generation (see below). By considering the dependence of photoluminescence spectra and dynamics on applied electric field, we develop here an alternative, unified description of the excitation dynamics at the polymer heterojunction. We show that in all blends the exciton first dissociates at the heterojunction and forms an interfacial geminate charge pair. However, geminate pair recombination via an intermediate heterojunction state (termed an exciplex) can regenerate the bulk exciton. These circular transitions between the different excited states at the heterojunction are driven by thermal energy, and a fine balance of the kinetics determines the net charge separation and photoluminescence yields.

Bulk excitons show relatively strong Coulombic binding (of order 0.5 eV [4, 8]), and can be trapped at the heterojunction, acquiring some charge-transfer character. Such excitations are termed exciplexes when seen in isolated donor-acceptor systems and are characterized by featureless, red-shifted emission spectra and long radiative decay times [9]. Recently, we have shown that exciplex states form in blends of F8BT with PFB, and F8BT with TFB (see Fig. 2 for molecular structures), and that these exciplex states can undergo endothermic energy transfer to form a bulk F8BT exciton [7]. Here we investigate films of PFB:F8BT and TFB:F8BT spin-coated from common chloroform solution. In general, there is substantial

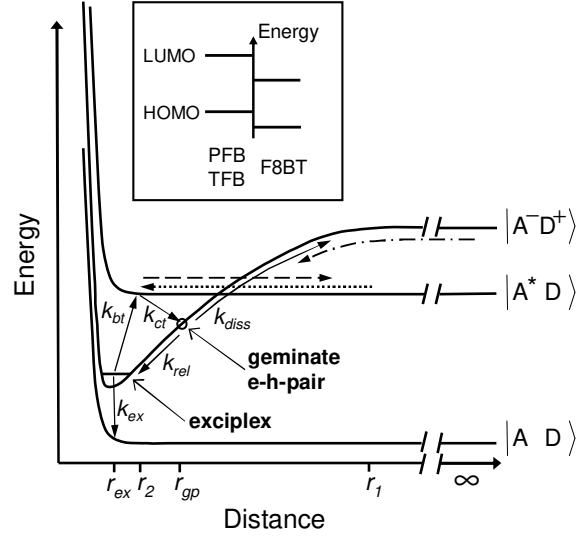


Figure 1: Potential energy diagram describing the energetics and kinetics at type II polymer heterojunctions. The energetic order of $|A^+D^-|_{r=1}$ and $|A^*D|_{r=1}$ may be reversed for PFB:F8BT vs. TFB:F8BT. The inset shows the band sets at a type II heterojunction (see also [7]).

demixing of the two polymers through spinodal decomposition during drying, but under the rapid drying conditions achieved here there is more limited demixing (of the order of 10 nm [2]) resulting in a large interfacial area of contact between the two polymers. Note that PFB:F8BT blends can display high charge separation yields (4% photocurrent external quantum efficiency) and low EL efficiencies ($< 0.64 \text{ lm/W}$) whereas the TFB:F8BT system displays low photocurrents (we find 82% lower short-circuit current than in PFB:F8BT at 457 nm excitation), but very high electroluminescence efficiencies (up to 19.4 lm/W) [7, 10]. Hence, these blends are good examples for the contrasting properties of type II polymer heterojunctions as described above.

For all measurements, polymer blends (mass ratio 1:1) were spin-coated from common chloroform solution onto oxygen-plasma-treated ITO substrates to form 170 nm thin films. Ca electrodes (60 nm) were then deposited by thermal evaporation and encapsulated by a 300 nm Al layer. All devices were fabricated under N_2 atmosphere. An electric field was applied by reverse-biasing the device to prevent charge injection (ITO negative with respect to Ca). Quasi-steady-state photoluminescence (PL) quenching measurements were taken by exciting the sample with a CW Ar^+ laser (457 nm) through the ITO. The resulting PL was imaged through a monochromator onto a Si photodiode. A modulated voltage

was applied to the device and changes in PL due to the applied electric field, PL, were detected using a lock-in amplifier referenced to the modulation frequency (225 Hz). The total PL intensity was measured by mechanical modulation of the laser excitation. The results reported here are independent of modulation frequency and excitation power. Time-resolved PL measurements were also performed using time-correlated single photon counting (TCSPC) and photoluminescence up-conversion (PLUC) spectroscopies with 70 ps and 300 fs time-resolution, respectively. Our TCSPC and PLUC setups are described elsewhere [7, 11]. All measurements were taken in continuous-flow He cryostats (Oxford Instruments OptistatCF) under inert conditions. Finally, PL efficiency measurements were performed on simple polymer thin films spin-coated on Spectrosil substrates using an integrating sphere coupled to an Oriel InstaSpec IV spectrograph and excitation with the same Ar⁺ laser as above.

Fig. 2 (a) compares the PL spectrum of a diode made with blended PFB:F8BT with that of pure F8BT. Red-shifted exciplex emission, in addition to bulk F8BT contribution (i.e. the F8BT-only spectrum), is evident in the blend film. (Neither PFB nor TFB are excited at 457 nm [10].) Also shown in the same figure is the PL spectrum taken by applying 10 V bias across the device. The electric field preferentially quenches the exciplex contribution in the red part of the spectrum (> 50% quenching for wavelengths > 650 nm). Quenching of the F8BT exciton emission is also observed, but decreases with decreasing temperature, as demonstrated in Fig. 2 (b). Similar phenomena are observed in the TFB:F8BT diode (Figs. 2 (c) and 2 (d)), although the relative contribution of F8BT bulk emission is higher in the same temperature range. In contrast to the blends, pure F8BT does not show PL quenching (integrated PL/PL ~ 1%) and only Stark-shifts by < 1 nm at these fields.

If the PL quenching arises from field-assisted dissociation of an emissive state, its luminescence decay rate should be field-dependent. Fig. 3 (a) shows TCSPC measurements at 640 nm in a PFB:F8BT diode with different applied voltages. All curves consist of an instrument-limited decay, and a slow, roughly mono-exponential decay with 40–5 ns time constant. The two components are assigned to the bulk exciton and the exciplex state, respectively [7]. Exciplex generation occurs within ~ 1 ns and its generation efficiency is strongly field-dependent, while its decay constant shows no significant variation with applied field. Therefore, an exciplex precursor must be quenched by the field. To investigate the field dependence on the bulk exciton decay rate, we have performed field-dependent PLUC

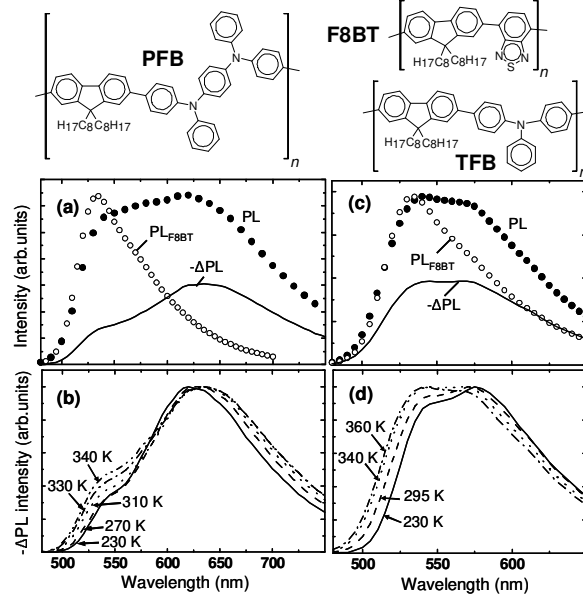


Figure 2: (a) Photoluminescence intensity (PL, solid circles) and reduction of photoluminescence intensity due to an applied reverse bias of 10 V (PL, continuous line) for a PFB:F8BT blend device at 340 K. PL and PL are plotted in the same scale and reflect their relative intensities. (b) PL spectra (at 10 V) from the same device as in (a) at different temperatures. (c) PL (solid circles) and PL at a reverse bias of 15 V (continuous line) for a TFB:F8BT blend device at 340 K. (d) PL spectra from the same device as in (c) at different temperatures. For comparison the PL spectrum from an F8BT-only device (open circles) is plotted in both part (a) and (c). The structures of PFB, F8BT, and TFB are also shown.

measurements. The results are displayed in Fig. 3(b). The exciton decay dynamics are not field dependent [12]. Therefore, a dark intermediate state must be dissociated by the field. We postulate that this state is an interfacial geminate polaron pair that follows charge transfer from the bulk exciton [13, 14, 15, 16].

To estimate the electron-hole separation within this geminate pair, r_{gp} , we have investigated the field-dependent changes in PL intensity (Fig. 4). Neglecting the effects of energetic disorder [17] and of a possible interfacial dipole layer [16], geminate-pair dissociation in electric fields is most easily described within the Onsager model [18], which yields the dissociation probability $f(r_{gp}; T; F) = f(F)$ of bulk geminate pairs in a medium with dielectric constant ϵ , under an applied field F and at temperature T [19]. Since the only material parameter is the dielectric constant, which we approximate to be 3.5 for all polymers, Onsager

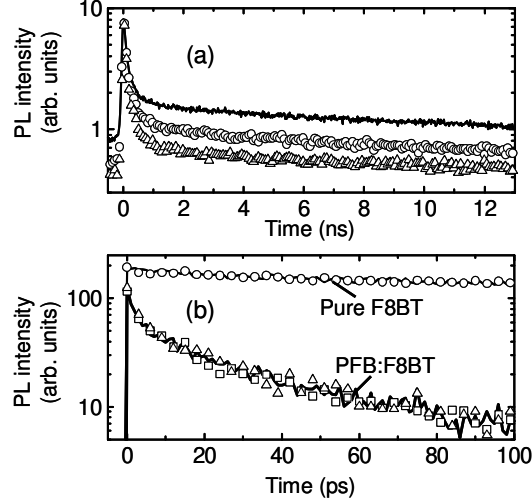


Figure 3: (a) Photoluminescence decay measured using TCSPC (excitation: 407 nm, $< 4 \text{ nJ/cm}^2$, detection: 640 nm) from a PFB:F8BT device at room temperature under 0V (continuous line), 13V (circles) and 30V (triangles) applied reverse biases. (b) PLUC measurements (excitation: 405 nm, 42 nJ/cm^2 , detection: 550 nm) from a similar device at 0V (continuous line), 5V (squares) and 12.5V (triangles) reverse bias. For comparison, data for a device with pure F8BT at 0V (continuous line) and 12V (circles) are also plotted.

theory should be applicable also to geminate pairs at the interface. The field-dependent relative reduction of the geminate pair population n_{gp} is given by $\frac{n_{gp}}{n_{gp}^0} = \frac{f(E) - f(0)}{1 - f(0)}$. Fig. 4 plots $\frac{P_L}{P_L^0}$ versus electric field [20] at various temperatures for PFB:F8BT and TFB:F8BT devices (measured in the red part of the spectrum where exciton emission is insignificant). Plotted in the same graph are simulations of $\frac{n_{gp}}{n_{gp}^0}$ using a δ -function distribution for r_{gp} . The simple model fits the data satisfactorily, which supports the assumption of a geminate pair intermediate prior to exciplex formation and yields $r_{gp} = 3.1 \text{ nm}$ (PFB:F8BT) and $r_{gp} = 2.2 \text{ nm}$ (TFB:F8BT). The large separation is probably caused by polaron-pair thermalization following the initial charge-transfer step [13, 18].

We now return to the PL spectra in Fig. 2, which contain bulk F8BT components that are not due to electric-field promoted dissociation of those states as was shown above. The zero-field steady-state photoluminescence is due to three different excited-state populations: (i) "primary" excitons, generated in the bulk by the laser excitation; (ii) exciplexes, generated via energy transfer from bulk excitons; and (iii) "secondary" excitons, generated via endothermic back-transfer from the exciplexes [7]. Since the exciplex density is reduced

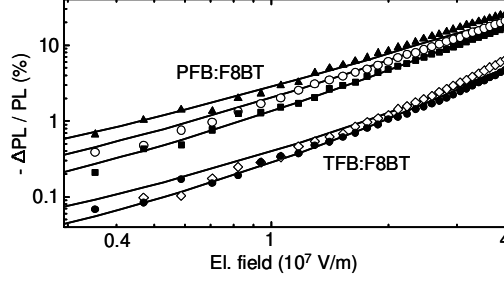


Figure 4: Relative electric field quenching of the PFB:F8BT and TFB:F8BT exciplex photoluminescence intensities (measured at 700 nm and 580 nm, respectively), in the same devices as in Fig. 2, versus electric field at 230 K (solid squares), 250 K (open and solid circles), 290 K (solid triangles) and 295 K (open diamonds). The solid lines through the data are Onsager simulations (parameters for PFB:F8BT: $\epsilon = 3.5$, $r_{gp} = 3.0$ nm at $T = 230$ K and 3.1 nm at 250 K and 290 K; for TFB:F8BT: $\epsilon = 3.5$, $r_{gp} = 2.3$ nm at $T = 250$ K and 2.2 nm at 295 K).

by application of an electric field, there is less secondary exciton generation, and hence the observed PL contains an excitonic contribution. Further evidence for this hypothesis is provided by the temperature dependence of the PL spectra shown in Figs. 2(b) and 2(d) [21]. The ratio of secondary excitons to exciplexes is found to follow an Arrhenius function with activation energy 200–50 meV (PFB:F8BT) and 100–30 meV (TFB:F8BT). These activation energies are consistent with those values extracted with our previous TC-SPC measurements [7].

Fig. 1 summarizes the above findings. The potential energy curves represent the ground state (A^+D), the exciton residing on F8BT (A^+D), and the electron and the hole residing in the respective component across the heterojunction (A^+D^+), where A and D symbolize the acceptor (F8BT) and the donor (PFB or TFB), respectively. The abscissa represents the intermolecular distance, i.e. either the distance of the exciton from the interface or the separation of the geminate polarons. The exciplex state is then located in the minimum of the A^+D^+ potential. When the system is photoexcited, an exciton is generated at a certain distance r_1 from the heterojunction. It then diffuses to a separation r_2 (dotted arrow), where it dissociates and an interfacial geminate electron-hole pair is formed with rate constant k_{ct} . This geminate pair can either dissociate (k_{diss}) or relax into the luminescent exciplex state (k_{rel}). The ratio k_{diss}/k_{rel} is strongly field dependent and determines the degree of luminescence quenching. The exciplex state can then either decay (k_{ex}), or back-transfer to

a bulk exciton in F8BT (k_{bt}), but is itself too strongly bound to dissociate under the field. We note that the transition from geminate pairs to excitons via $k_{rel} \rightarrow k_{bt}$ represents a novel mechanism for geminate pair recombination at polymeric heterojunctions. The secondary excitons produced might enter the cycle again, or diffuse away from the heterojunction (dashed arrow) and decay. The model is also applicable to electrical excitation, where the excited state is produced via charge injection (dash-dotted arrow). The regeneration of the exciton via the thermally-driven circular process $k_{ct} \rightarrow k_{rel} \rightarrow k_{bt}$ means that even though charge transfer occurs, the excitation energy might eventually still be emitted in the form of bulk exciton luminescence.

An estimate of the contribution of the regeneration process to the PL of the blend can be derived by normalizing the PL spectrum to the PL spectrum at higher wavelengths where the emission is solely due to exciplexes. We assume that this re-normalized PL then represents the contribution of exciplex and secondary exciton emission to the total PL. We infer thereby that at room temperature in the PFB:F8BT blend ~20% of the visible emission comes from primary excitons. In TFB:F8BT we find a primary exciton contribution of < 2%, which implies that > 98% of the excitons undergo charge transfer at a heterojunction. Despite that, the relative PL quenching with respect to pure F8BT is only < 57% (PL yield of F8BT 80%, of TFB:F8BT 35%) indicating the great importance of the exciton regeneration mechanism. Secondary exciton and exciplex emission maintain a high PL yield in spite of most excitons encountering a heterojunction. On the other hand, the PFB:F8BT PL yield is only 4%, consistent with large geminate pair dissociation and low back-transfer efficiency, i.e. with low "regeneration efficiency".

In summary, we have developed a comprehensive description of the excitonic and electronic processes at type-II polymer heterojunctions that support exciplex formation. The two blends studied here represent important examples for efficient charge generation on the one hand and high luminescence yields on the other, and in this sense represent the two extremes of type-II heterojunctions found in common semiconductor polymer blends. The very different behavior was shown to arise from different geminate pair separations (3.1 nm vs. 2.2 nm) and back-transfer activation energies (200 meV vs. 100 meV) which affect strongly the kinetics between the states involved. We note that both thermalization distance as well as activation energy are generally expected to be larger for larger band edge offsets between the two polymers and that this provides the link to the classification scheme described in

the introduction [4]. Given that excited-state electronic dimers are commonly observed in polymeric semiconductors [22], we consider exciplex formation and exciton regeneration to also be general phenomena at type II polymeric heterojunctions. As shown in this letter, the central role of these dynamics is not directly evident from steady-state PL measurements if back-transfer is efficient.

In photovoltaic operation the collapse of the geminate pair into the exciplex provides an unwanted loss channel. We suggest that optimized interfaces require not only large band-edge offsets to enable large thermalization distances (τ_{sp}), but also inhibited exciplex stabilization. This can be achieved by increasing intermolecular distances and decreasing configurational relaxation [9].

This work was supported by the EPSRC. ACM is a Gates Cambridge Scholar. CS is an EPSRC Advanced Research Fellow. We are grateful to N.C. Greenham and A.S. Dhoot for valuable discussions.

Current address: Clarendon Laboratory, University of Oxford, Parks Road, Oxford OX1 3PU, United Kingdom

^y Corresponding author. E-mail: cs271@cam.ac.uk

- [1] J. J. M. Halls et al, Nature 376, 498 (1995).
- [2] A. C. Arias et al, Macromolecules 34, 6005 (2001).
- [3] C. J. Brabec, N. S. Sariciffci, and J. C. Hummelen, Adv. Funct. Mater. 11, 15 (2001).
- [4] J. J. M. Halls et al, Phys. Rev. B 60, 5721 (1999).
- [5] Y. Cao et al, Nature 397, 414 (1999).
- [6] L. C. Palilis et al, Synth. Met. 121, 1729 (2001).
- [7] A. C. Mordeani et al, Adv. Mat. 15, 1708 (2003).
- [8] S. Alvarado et al, Phys. Rev. Lett. 81, 1082 (1998).
- [9] A. Weller, in The Exciplex, edited by M. Gordon and W. Ware (Academic Press Inc., New York, 1975), pp. 23-38.
- [10] H. J. Snaith et al, Nano Lett. 2, 1353 (2002).
- [11] G. R. Hayes et al, Phys. Rev. B 52, 11569 (1995).
- [12] We note that field-assisted exciton dissociation has been seen in a related polyurene at

- higher fields (see T. Virgili et al., Phys. Rev. Lett. 90, 247402 (2003)).
- [13] M. Yokoyama et al., J. Chem. Phys. 75, 3006 (1981).
- [14] M. W. Wu and E. M. Conwell, Chem. Phys. 227, 11 (1998).
- [15] N. Ohta, Bull. Chem. Soc. Jpn. 75, 1637 (2002).
- [16] V. I. Arkhipov, P. Heremans, and H. Bassler, Appl. Phys. Lett. 82, 4605 (2003).
- [17] V. R. Nikitenko, D. Hertel, and H. Bassler, Chem. Phys. Lett. 348, 89 (2001).
- [18] M. Pope and C. E. Swenberg, Electronic Processes in Organic Crystals and Polymers (Oxford University Press, 1999), 2nd ed.
- [19] $f(r_{gp}; T; F) = \frac{1}{2} \int_0^R d \sin e^{(A+B)} \sum_{m=0}^P \frac{A^m}{m!} \frac{B^{m+n}}{(m+n)!}; A = 2q r_{gp}, B = r_{gp}(1 + \cos \theta),$
 $q = e^2/8 \epsilon_0 kT, \quad \theta = eF/2kT$ (see ref. [18], p. 484). Averaging over θ represents an isotropic blend morphology.
- [20] Internal field calculated as $F = (\text{applied Voltage} + x)/170 \text{ nm}$; x is the Voltage corresponding to minimum PL=PL, found to be 0.7V (PFB F8BT) and 0.3V (TFB F8BT) forward bias.
- [21] At temperatures below 230 K the PL arising from the excitons' Stark-shift obscures the weak quenching signal.
- [22] B. J. Schwartz, Annu. Rev. Phys. Chem. 54, 141 (2003) and references therein.